

Erratum: Unexpected softness of bilayer graphene and softening of A-A stacked graphene layers [Phys. Rev. B 101, 125421 (2020)]

Y. W. Sun,^{1,*} D. Holec,^{2,†} D. Gehringer,² O. Fenwick,¹ D. J. Dunstan,³ and C. J. Humphreys¹

¹*School of Engineering and Materials Science, Queen Mary University of London, London E1 4NS, United Kingdom*

²*Department of Materials Science, Montanuniversität Leoben, Leoben 8700, Austria*

³*School of Physics and Astronomy, Queen Mary University of London, London E1 4NS, United Kingdom*

(Dated: February 12, 2021)

I. ERRATUM PROPER

There are quantitative errors in Figs. 1 and 2 of our paper,[1] affecting its first conclusion. Stress evaluation employing the Vienna *Ab initio* Simulation Package (VASP) on inhomogeneous structures, and in particular on structures where internal strain occurs, requires special handling. [Bilayer graphene is such a structure, with a large vacuum separation in the supercell along the \$c\$ -axis perpendicular to the graphene plane. We misinterpreted the stress presented in the original Fig. 1 as the stress on the graphene layers. We correct the stress in Fig. 1 below, by a simple scaling following the approach in the literature.\[2, 3\] The key message is qualitatively consistent with the original paper, that bilayer graphene stiffens more slowly than graphite, over the compression range before the rehybridization of \$sp^2\$ to \$sp^3\$ \(*i.e.* the curve of stress against interlayer spacing of bilayer is shallower than graphite in this range\).](#) Additionally, a systematic error in integrating the charge density influenced the discussion of the charge between graphene layers. This error is corrected in Fig. 2 and its impact is discussed in the corresponding text below. Despite the errors arising from these methodological mishandlings, the original interpretation and conclusions remain qualitatively unchanged.

We modeled bilayer graphene by having two layers of graphene in a large supercell with a fixed height $Z = 24.65 \text{ \AA}$ (for a large vacuum separation) along the c -axis perpendicular to the graphene layers. The graphene layers were at a variable spacing d , and the remainder of the space in the supercell was vacuum. The first derivative of the total energy of the supercell with respect to a displacement \mathbf{q} , [evaluated at \$\mathbf{q} = 0\$](#) , gives the magnitude of the force \mathbf{F} . The type of displacement determines what force we obtain. For example, the displacement of a carbon atom along the c -axis yields the force on that atom along this direction; the displacement of the whole graphene plane along the c -axis gives the force, and hence the stress, on that plane. The stress tensor evaluated by VASP by default is the stress on the supercell, evaluated with \mathbf{q} being the deformation of the supercell as a whole, *i.e.* including its contents. That is, the strain

between any two atoms inside the supercell is the same (affine displacements). Unless the system is then relaxed (equilibrated), before the calculation of the change in energy, results for inhomogeneous systems or systems with internal strain are incorrect.

With our large vacuum separation, we expect the stress σ_{33} along the c -axis on the supercell to be zero. As it was not zero, we misinterpreted it as the stress on the graphene. Indeed, the energy change was not large, as the graphene separation changed by the factor d/Z less than the change in the height of the supercell, where d is the each fixed distance between the layers in bilayer graphene. Interestingly, Munet and Marzari obtained $c_{11} + c_{12}$ of graphite from the second differential of energy with respect to biaxial strain, but they did not get c_{11} or c_{12} in this way, as the required strains cause internal strain in the four-atom unit cell.[4] Instead, they obtained them from phonon dispersions. Liu *et al.* also explicitly state the need for the graphene structure to be relaxed after every deformation before calculating the Young's modulus and Poisson's ratio.[2] On the other hand, they did use the stress on the supercell containing graphene and vacuum, which they referred to as a stress *averaged* over the supercell volume. They therefore corrected it by the factor Z/d_0 for calculating the stress on the graphene from the supercell stress. [Capaz *et al.* used a similar approach to evaluate the stress along a carbon nanotube axis after straining the tube along this direction, by a scaling factor of the length of the unit cell in the dimension with a large vacuum separation \(to model an individual tube\), over the diameter of the tube cross section.\[3\] Although the bilayer graphene is under internal strain \(except at equilibrium\), the stress on the layers can be directly evaluated by VASP \(from affine displacements\) with a scaling factor, because the contribution of a small deformation of the large vacuum \(height over 20 Å\) to the total energy is negligible. In Fig. 1, we present the stress corrected by multiplying by the factor \$Z/d\$.](#)

The corrected figure shows that for both Bernal (AB) and AA stackings, to compress to smaller interlayer distance, the required uniaxial stress along the c -axis increases more slowly on a bilayer graphene than graphite. This key conclusion is consistent with the original paper.

The error in the original Fig. 2 is more subtle: the integrated charge density suffered from numerical issues. The charge density is calculated on a grid, sampling the whole simulation cell, *i.e.* it is known only as a discrete quan-

* yiwei.sun@qmul.ac.uk

† david.holec@unileoben.ac.at

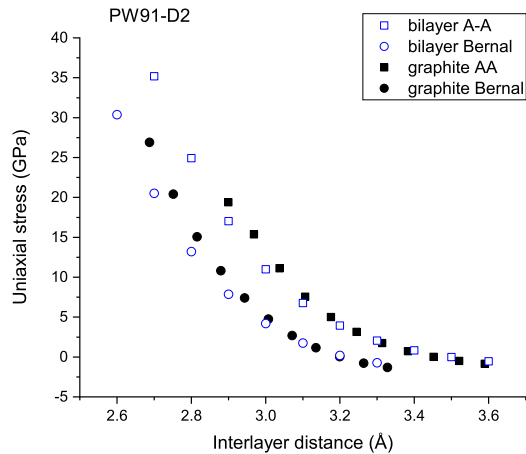


FIG. 1. Corrected Fig. 1 by simply multiplying a scaling factor. The uniaxial stress along the c -axis applied to A-A and Bernal stacked bilayer graphene and graphite is plotted with the corresponding interlayer distance at which the stress was calculated. The black solid points are for graphite, and the blue open circles are for bilayer graphene. Circles are for Bernal stacking, and squares are for A-A.

tity. The chosen step for sampling the bilayer interlayer distance (of 0.1 \AA) was not commensurate with the simulation box dimension (of 24.65 \AA) and grid size (of 500 points). Therefore, whereas one graphene layer (at $z = 0$) always remained at a charge density grid point, the other layer “moved” to different relative positions between two grid points. As our fast Fourier transform (FFT) grid-spacing in the z -direction is $\Delta_{\text{CFFT}} = 0.0493 \text{ \AA}$, moving a plane over a distance of 0.1 \AA means moving it by 2 FFT grid points plus an offset $\Delta_{\text{Coff}} = (0.1 - 2\Delta_{\text{CFFT}})/\Delta_{\text{CFFT}}$ which calculates to be $\approx 2.8\%$ of Δ_{Coff} . Consequently, the (numerically) integrated charges suffered from systematic errors, since the values of ρ (within the PAW (the projector augmented wave method, for near-core valence wavefunctions) spheres) on the FFT grid are sensitive to their distance from the atomic centers, resulting in largely overestimated charge density changes. We now fix the relative position of the graphene layer to the grid points. The corrected valence charge between graphene layers at various interlayer distances is presented in Fig. 2, replacing the old Fig. 2. Electrons are squeezed through graphene planes for both Bernal and AA stacked bilayer graphene, where the original interpretation applies: This unexpected softness is related to the possibility of electrons being squeezed through graphene planes.

Due to the same error in Fig. 1, the Fig. 1 in the supporting information (SI) is corrected and replaced by Fig. 3 with the corrected values of the stress. The message is unchanged that in-plane phonon frequencies shift non-monotonically in an A-A stacked bilayer, suggesting a large disruption of the sp^2 -orbital distribution under out-of-plane compression, in addition to electrons being

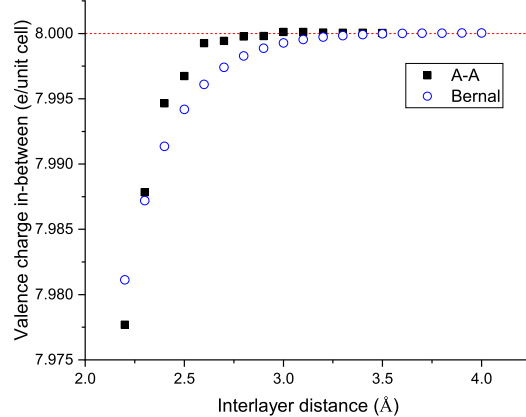


FIG. 2. Corrected Fig. 2. The integrated valence charge between the two graphene layers is plotted versus the interlayer distance of bilayer graphene for A-A (blue open circles) and Bernal stacking (black solid squares). The horizontal dashed line is for graphite.

squeezed through the graphene plane discussed above. A further correction is that in the caption of Fig. 5, ‘bilayer graphene’ should be replaced by ‘graphite’.

In conclusion, we have corrected the results of the first part of the original paper. **The key message that bilayer graphene stiffens more slowly than graphite along the c -axis perpendicular to the graphene plane (*i.e.* the stress increases more slowly with decreasing interlayer spacing in bilayer) is unchanged. The quantitative description has been corrected.** The proposed mechanism, that this softness is related to the possibility of electrons being squeezed through graphene layers, is also unchanged.

II. VDWS CORRECTIONS

Fig. 4 demonstrates that the choice of vdW corrections does not affect our key message that bilayer graphene stiffens more slowly than graphite. We interpolate the data of Bernal stacked graphite in Fig. 1 (black circles). We obtain the interlayer potential at a interlayer distance, by integrating uniaxial stress along the c -axis over interlayer distance, from the calculated distance at equilibrium, to this distance. We use the Lennard-Jones (LJ) potential in the AB form, with a vertical offset to make the energy minimum at zero:[5] $V_{LJ}(r) = \frac{A}{r^{12}} - \frac{B}{r^6} + C$, to fit the interlayer potential. The fit (orange solid line) almost overlaps with the data (black solid lines). We then plot the modified LJ potential by increasing or decreasing the attraction coefficient B by 10%, while fixing the repulsion coefficient A and offset C at the fitted values (two orange dashed lines, respectively to the increased and decreased B). We compare the interlayer potential of graphite with its attraction term modified, to that of

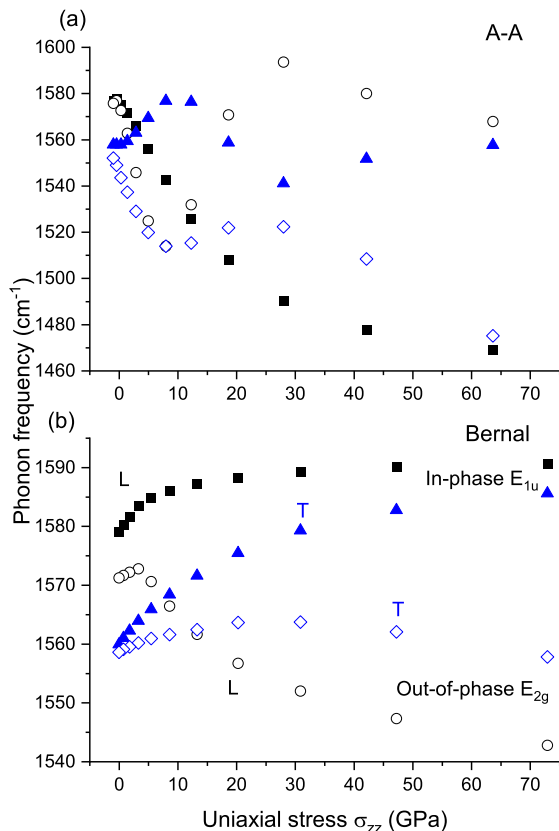


FIG. 3. Corrected Fig. 1 in the SI. The caption remains the same: The frequencies of the 4 in-plane phonons of A-A (a) and Bernal (b) stacked bi-layer graphene are plotted with uniaxial stress along the c -axis. The solid points are for the two-plane in-phase modes (E_{1u}) and the open points are for the two-plane out-of-phase modes (E_{2g}). The black points are for the modes along the longitudinal direction in the hexagonal plane of graphene (L) and the blue points are for the modes along the transverse direction (T).

bilayer graphene.

The message is clear, that the attraction term affects the energy minimum and the interlayer distance at equilibrium, but not the curvature of the interlayer potential-distance relation, and therefore the choice of vdW corrections cannot be responsible for the separation between graphite and bilayer graphene in the compressibility behaviour shown here.

We do not intend to argue which correction is superior to another, in better describing the vdW, determining the interlayer spacing at equilibrium, because equilibrium position is not a concern of this paper. Therefore, the comparison of the elastic constant c_{33} at equilibrium between graphite and bilayer graphene in the original paper was misleading. The relevant parameter is the variation of the out-of-plane stiffness, the curvature of the interlayer stress-distance relation, presented in Fig. 1.

- [1] Y. W. Sun, D. Holec, D. Gehringer, O. Fenwick, D. J. Dunstan, and C. J. Humphreys, Unexpected softness of bilayer graphene and softening of a-a stacked graphene layers, *Phys. Rev. B* **101**, 125421 (2020).
- [2] F. Liu, P. Ming, and J. Li, *Ab initio* calculation of ideal strength and phonon instability of graphene under tension, *Phys. Rev. B* **76**, 064120 (2007).
- [3] R. B. Capaz, C. D. Spataru, P. Tangney, M. L. Cohen, and

- S. G. Louie, Hydrostatic pressure effects on the structural and electronic properties of carbon nanotubes, *physica status solidi (b)* **241**, 3352 (2004).
- [4] N. Mounet and N. Marzari, First-principles determination of the structural, vibrational and thermodynamic properties of diamond, graphite, and derivatives, *Phys. Rev. B* **71**, 205214 (2005).
- [5] J. E. Lennard-Jones, Cohesion, *Proc. Phys. Soc.* **43**, 461 (1931).

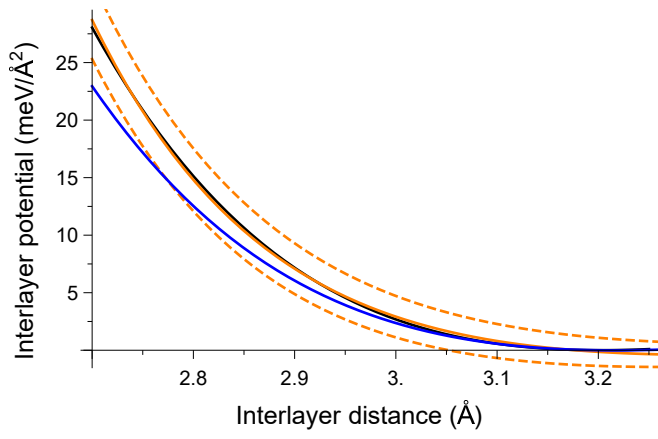


FIG. 4. The interlayer potential of Bernal stacked graphite and bilayer graphene is plotted with interlayer distance. The black line is the data for graphite. The orange solid line is the fit using LJ potential (almost overlapping with the data). The orange dashed lines are modified LJ potential with 10% increased or decreased attraction coefficient, respectively, while the repulsion is the same as the orange solid line. The blue line is the data for bilayer graphene.